
INVOLUTION GAME WITH MIGRATION AND SPATIAL HETEROGENEITY OF SOCIAL RESOURCES

A PREPRINT

Bo Li^{*1}, Qiwen Ge^{†1}, and Yong Shi^{‡2,3,4}

¹School of Finance and Economics, Wuhan City Polytechnic, Wuhan 430064, China

²School of Economics and Management, University of Chinese Academy of Sciences, Beijing 100190, China

³Research Center on Fictitious Economy and Data Science, Chinese Academy of Sciences, Beijing 100190, China

⁴Key Laboratory of Big Data Mining and Knowledge Management, Chinese Academy of Sciences, Beijing, 100190, China

March 16, 2026

ABSTRACT

Involution—a phenomenon of excessive competition with diminishing returns—has become a pressing socio-economic concern in contemporary China, prompting both academic inquiry and policy interventions. This paper proposes an evolutionary game model of involution that incorporates agent migration and spatial heterogeneity in resource distribution. The model captures realistic features such as effort-based resource allocation, local interactions on a lattice, and mobility driven by payoff comparisons. We explore how varying conditions of migration and resource allocation influence the dynamics of involution. The key findings from our simulations are as follows: when total resources are held constant, similar resource levels across different regions tend to suppress involution; conversely, an increase in total resources exacerbates it. In addition, the probability of migration does not significantly affect the final evolutionary outcome. We further identify threshold effects in the effort ratio and utility multiplier, revealing critical conditions under which involution emerges or subsides. To further elucidate these simulation results, we conduct a theoretical analysis using mean-field theory, which provides analytical expressions for the equilibria and stability conditions. The theoretical predictions are in excellent qualitative agreement with simulation outcomes. Finally, we discuss real-world counterparts of the model, including competition among food delivery riders and between stores offering similar services.

Keywords Involution · Migration · Resource heterogeneity · Evolutionary game · Agent-based model

1 Introduction

The term “involution” actively discussed in the contemporary Chinese context refers to a phenomenon of excessive competitive behavior under conditions of limited resources, characterized by diminishing returns on individual efforts despite increased inputs [1, 2]. This socio-economic pattern has been observed across various domains, including labor markets, education, and commercial competition, where participants engage in escalating effort without proportional gains. Recently, in response to the recognized impediments posed by involutory competition, China has implemented policy interventions aimed at mitigating its adverse effects on socio-economic advancement [3]. Understanding the mechanisms driving involution is therefore crucial for designing effective policies.

At its core, involution shares structural similarities with classic social dilemmas such as the prisoner’s dilemma [4, 5, 6, 7] and the public goods game [8, 9, 10]—foundational concepts in game theory that capture the tension

*libo312@mailsucas.ac.cn

†597251335@qq.com, corresponding author.

‡yshi@ucas.ac.cn

between individual rationality and collective welfare. This structural similarity has motivated researchers to employ evolutionary game theory—a well-established framework for analyzing strategic interactions—to examine the dynamics of involution, providing mechanistic insights into its emergence and potential pathways for mitigation [11, 12, 13, 14].

Building on these foundational insights, Wang et al. [2] proposed a spatially explicit model on a square lattice where agents choose between two strategies distinguished by effort levels. Resources are allocated according to a maximum entropy principle, and agents adjust their strategies based on payoff comparisons with neighbors. Using the adoption ratio of the high-effort strategy as an indicator of involution intensity, they found that more abundant social resources can paradoxically intensify involution, while increased stochasticity in resource allocation suppresses it; moreover, the cost of high effort exhibits non-monotonic effects on involution dynamics.

In subsequent work, Wang et al. [11] extended the model to incorporate spatio-temporal heterogeneity in social resources. They found that spatial heterogeneity has a dual effect on involution: it mitigates competition when resources are abundant (via network reciprocity), but intensifies it under moderate resource levels. Temporal heterogeneity, however, erases these spatial effects and restores homogeneous-population dynamics. Meanwhile, Li [12] introduced a specialization strategy wherein agents concentrate efforts on specific resource niches, revealing that the adoption of specialization depends intricately on resource abundance, effort costs, and stochasticity.

Beyond these involution-specific models, broader evolutionary game research has illuminated how spatial structure and updating rules especially migration affect cooperation [15, 16, 17, 18, 19, 20, 21, 22, 23]. For instance, the interplay between local and global strategy updating in public goods games significantly influences cooperative outcomes [15]. More importantly for our purposes, migration based on environmental comparison has been shown to promote cooperation in evolutionary games [16], highlighting the importance of mobility in strategic evolution. This observation motivates the central question of our study: how does agent mobility interact with spatial resource heterogeneity to shape involution dynamics?

Despite the advances in involution modeling, existing evolutionary game models have largely neglected agent mobility—a critical feature of many real-world competitive contexts. In reality, delivery workers, couriers, and homogeneous stores often compete for limited resources within regions while retaining the ability to relocate to areas with more favorable effort-to-reward ratios. This mobility can fundamentally alter competitive dynamics, by redistributing competitive pressure across space and enabling agents to escape locally saturated markets, yet remains unexamined in current involution models.

To address this gap, we propose an evolutionary game model of involution that incorporates agent migration and spatial heterogeneity of social resources. Our model examines how varying levels of mobility and resource distributions influence involutionary outcomes, with direct applications to competitions among food delivery riders and homogeneous stores. The key findings from our simulations are as follows: when total resources are held constant, similar resource levels across different regions tend to suppress involution; conversely, an increase in total resources exacerbates it. In addition, the probability of migration does not significantly affect the final evolutionary outcome. Complementing these simulation results, we conduct a mean-field theoretical analysis [24, 25, 26] that reveals the underlying mechanisms driving these patterns. The analysis demonstrates that migration dynamics are governed by resource disparities, inevitably concentrating agents in resource-rich regions, while strategy evolution exhibits threshold behavior determined by average resource levels. Importantly, the theoretical predictions align closely with our simulation observations, confirming that the presence or absence of migration—rather than its precise rate—is the critical factor, and that total resource abundance fundamentally modulates involution intensity.

The remainder of this paper is organized as follows: Section 2 introduces the model formulation; Section 3 presents simulation results and analysis; Section 4 provides theoretical analysis to uncover underlying mechanisms; and Section 5 offers discussion and concluding remarks.

2 Model

We consider an $N \times N$ two-dimensional lattice with periodic boundary conditions to eliminate boundary effects. Each lattice site (x, y) may be occupied by at most one agent. The resource endowments are spatially heterogeneous: the lattice is divided into two equal halves with distinct resource levels M_1 (upper half) and M_2 (lower half), represented by a matrix \mathbf{M} where

$$m_{ij} = \begin{cases} M_1 & \text{for } i \leq N/2, \\ M_2 & \text{for } i > N/2, \end{cases}$$

The total number of agents is fixed at N_{agents} , yielding an initial occupation density $\rho = N_{\text{agents}}/N^2$.

2.1 Agent Strategies and Utility

Each agent adopts one of two strategies, characterized by effort levels and corresponding utilities:

- **Strategy C (low effort):** Effort level e_C , utility $u_C = e_C$.
- **Strategy D (high effort):** Effort level e_D , utility $u_D = \beta e_D$, where $\beta \geq 0$ is a multiplier that scales the utility of high effort relative to low effort.

The strategy of agent i at time t is denoted $S(i, t) \in \{C, D\}$, with associated effort $o(i, t)$ and utility $u(i, t)$ given by:

$$o(i, t) = \begin{cases} e_C, & \text{if } S(i, t) = C, \\ e_D, & \text{if } S(i, t) = D, \end{cases} \quad \text{and} \quad u(i, t) = \begin{cases} u_C, & \text{if } S(i, t) = C, \\ u_D, & \text{if } S(i, t) = D. \end{cases} \quad (1)$$

2.2 Payoff Calculation

At each time step, every agent competes for resources at five locations: its own site and its four nearest neighbors (von Neumann neighborhood with periodic boundaries). In each of these five independent competitions, the agent invests its entire effort e_i (where i denotes the agent's strategy) and bears the full cost e_i . The resource $M(j)$ at site j is divided among all agents whose neighborhoods include j (i.e., the agent at j and its four neighbors) in proportion to their efforts. Hence, the share obtained by agent i from site j is $\frac{e_i}{\sum_{k \in \mathcal{N}(j)} e_k} M(j)$, where $\mathcal{N}(j)$ denotes the set consisting of site j and its four neighbors. The denominator $\sum_{k \in \mathcal{N}(j)} e_k$ sums the efforts of all agents competing at site j ; because each agent contributes its full effort, this sum reflects the total competitive pressure at that location. After all five competitions, agent i 's payoff is the average net gain:

$$\pi(i, t) = \frac{1}{5} \sum_{j \in \mathcal{N}(i)} \left(\frac{e_i}{\sum_{k \in \mathcal{N}(j)} e_k} M(j) - e_i \right), \quad (2)$$

where $\mathcal{N}(i)$ is defined analogously. The factor $1/5$ normalizes the total net gain from five competitions to a per-competition average. Note that although the agent incurs a cost e_i in each competition, the total cost over five competitions is $5e_i$, so the average cost subtracted in Eq. (2) is e_i , correctly representing the per-competition cost.

2.3 Strategy Update Rule

At each discrete time step t , a pair of distinct agents (i, i') is randomly selected without replacement, where i is the focal agent and i' is the comparison agent. The probability that agent i adopts the strategy of agent i' at the next time step $t + 1$ is given by the Fermi function [27, 28]:

$$P(S(i, t + 1) = S(i', t)) = \frac{1}{1 + \exp([\pi(i, t) - \pi(i', t)]/k)}, \quad (3)$$

where $k \geq 0$ is the selection intensity (noise level). When $k \rightarrow 0$, the function approaches a step function: if $\pi(i, t) > \pi(i', t)$, the probability of adopting i' 's strategy is 0; if $\pi(i, t) < \pi(i', t)$, it is 1. Thus imitation becomes deterministic, always copying the strategy with the higher payoff. As k increases, the decision becomes more stochastic, allowing occasional adoption of lower-payoff strategies. This rule captures the stochastic nature of social learning while preserving a bias toward higher payoffs.

2.4 Migration Rule

Following the strategy update, the same pair (i, i') is used to determine a possible migration. Agent i may move to a location adjacent to agent i' , reflecting a tendency to cluster near successful individuals. Specifically, agent i randomly selects one of the four neighboring sites of agent i' (von Neumann neighborhood). If that site is empty, agent i migrates there at time $t + 1$ with probability:

$$P_{\text{migrate}} = \frac{\mu}{1 + \exp([\pi(i, t) - \pi(i', t)]/k)}, \quad (4)$$

where $\mu \in [0, 1]$ is the migration rate parameter controlling the baseline propensity to migrate. The same Fermi function appears here because migration, like strategy imitation, is influenced by payoff comparison: agents are more inclined to move toward those who outperform them. The factor μ scales the overall migration probability; if $\mu = 0$, migration never occurs, while $\mu = 1$ gives the full Fermi probability. The requirement that the target cell be empty prevents multiple agents from occupying the same site and ensures that population density remains bounded. If the selected neighbor of i' is occupied, the migration attempt fails and agent i remains at its current location.

2.5 Simulation Parameters

Table 1 summarizes the parameters used in our simulations, including their default values and the ranges explored. Each simulation was run for 3000 Monte Carlo steps, and the results were averaged over 50 independent realizations. For runs that did not reach an absorbing state within 3000 steps, the average over the last 300 steps was taken as the final outcome.

Table 1: Simulation parameters and default values.

Parameter	Description	Default value / Range
N	Lattice size (grid dimension)	100
N_{agents}	Total number of agents	2000 (varied in Sec. 3.7)
ρ	Initial agent density (N_{agents}/N^2)	0.2
e_C	Effort level of strategy C	0.1
e_D	Effort level of strategy D	0.2
β	Utility multiplier for strategy D ($u_D = \beta e_D$)	1 (varied in Sec. 3.4)
u_C	Utility of strategy C ($= e_C$)	0.1
u_D	Utility of strategy D ($= \beta e_D$)	0.2 (when $\beta = 1$)
k	Selection intensity	1 (varied in Sec. 3.1)
μ	Migration rate	0 to 1 (varied)
M_1, M_2	Resource levels in the two regions	$M_1 + M_2$ fixed at 2.0, 3.0, or 5.0; ratio varied

3 Results and Discussion

We systematically investigate how resource heterogeneity and agent mobility shape involutionary dynamics. The main observable is F_D , the fraction of agents adopting the high-effort strategy D. We also monitor the spatial distribution P_{M_1} , the proportion of agents located in the M_1 region.

3.1 Joint effects of migration and selection intensity

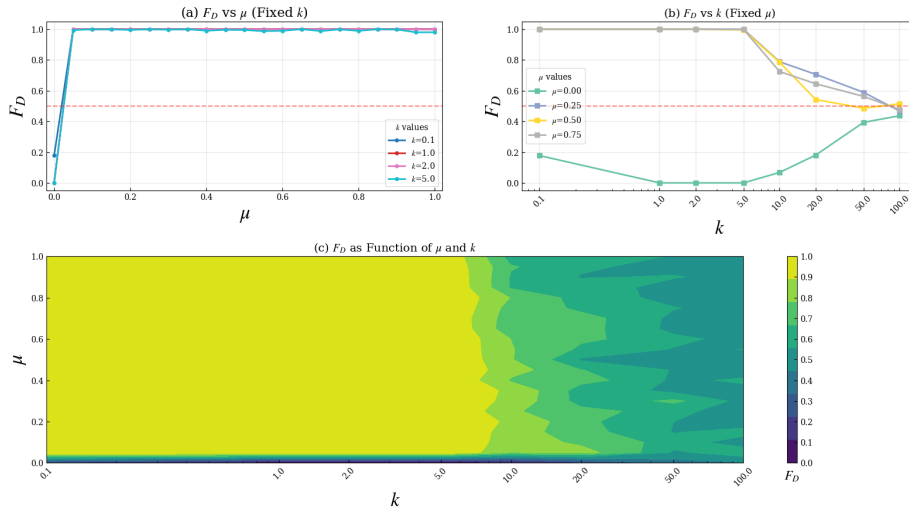


Figure 1: Proportion of competitive agents (F_D) as a function of migration rate μ and selection intensity k under asymmetric resource distribution ($M_1 = 1, M_2 = 2$). (a) F_D vs. μ for different k ; (b) F_D vs. k for different μ ; (c) contour plot over the whole parameter space. Averaged over 50 independent runs on a 100×100 lattice with 2000 agents. For runs not reaching an absorbing state within 3000 steps, the last 300 steps are averaged.

We first analyze the proportion of competitive agents adopting the high-effort strategy (F_D) across varying migration rates (μ) and selection intensities (k). Figure 1 elucidates the complex interplay between migration and selection intensity in determining involution levels under resource asymmetry ($M_1 = 1, M_2 = 2$).

Panel (a) reveals that the presence of migration (any $\mu > 0$) strongly suppresses competitive behavior compared to the immobile case ($\mu = 0$) regardless of whether k is 0.1, 1, 2, or 5. However, once migration is allowed, the exact value of μ has little effect on F_D across all selection intensities. Panel (b) further illustrates that when k exceeds a certain threshold (approximately $k = 5$), F_D gradually converges toward 0.5 as k increases. The contour plot (c) synthesizes these trends, highlighting three distinct regimes: (1) an immobile ($\mu = 0$) and low k regime characterized by low F_D (low involution); (2) a mobile ($\mu > 0$) and low- k regime characterized by high F_D (high involution); and (3) a regime at sufficiently large k where F_D gradually converges toward 0.5 with increasing k , irrespective of the migration rate. A more nuanced observation is that at intermediate selection intensities ($k \approx 10-30$), increasing μ yields a modest additional suppression of the high-involution state, even after migration is introduced.

In summary, the migration rate μ plays a moderating role whose strength depends on k : at low k , the presence of migration (any $\mu > 0$) dramatically alters the outcome; at intermediate k , higher μ further suppresses involution; at high k , the system converges to a balanced equilibrium ($F_D \approx 0.5$) regardless of μ . These findings highlight that the mere existence of mobility, rather than its precise rate, is the dominant factor except in a narrow intermediate regime.

3.2 Emergent spatial distribution of agents

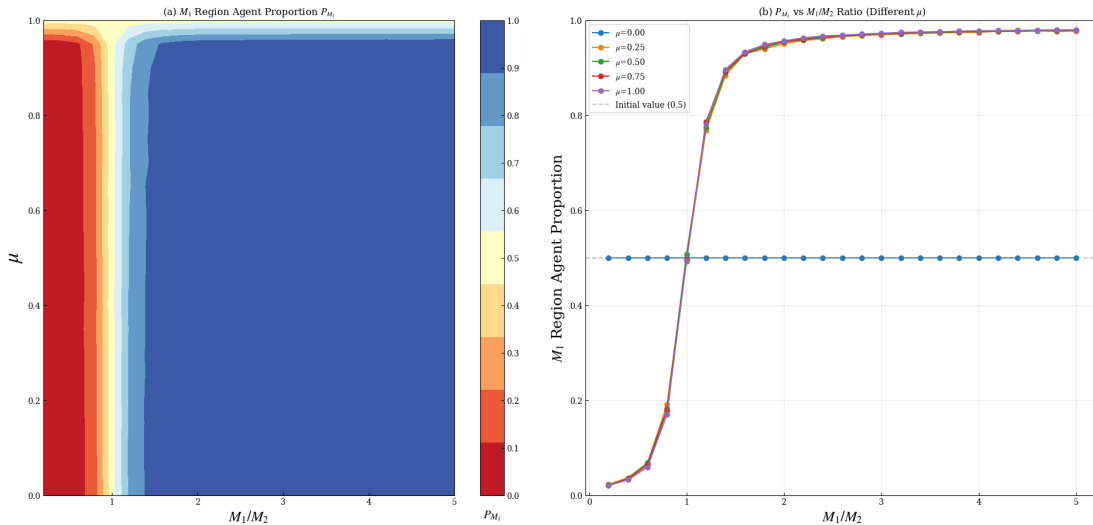


Figure 2: Proportion of agents located in region M_1 , P_{M_1} , as a function of the resource ratio M_1/M_2 for different migration rates μ . Simulations with total resources $M_1 + M_2 = 3.0$, 2000 agents on a 100×100 lattice, averaged over 50 independent runs. The dashed line at $P_{M_1} = 0.5$ indicates uniform distribution.

Figure 2 examines how agents distribute themselves between the two regions in response to resource asymmetry and migration opportunities under a moderate total resource level ($M_1 + M_2 = 3.0$). When migration is absent ($\mu = 0$), agents remain uniformly distributed ($P_{M_1} = 0.5$) for all M_1/M_2 , confirming that without mobility, spatial sorting does not occur. Once migration is allowed, agents rapidly concentrate in the resource-richer region. At $\mu = 1.0$, a modest resource advantage of $M_1/M_2 = 1.5$ drives P_{M_1} to approximately 0.90, while at $M_1/M_2 = 2.0$, P_{M_1} reaches 0.96. The concentration intensifies with both μ and the degree of asymmetry, approaching complete agglomeration ($P_{M_1} \rightarrow 1$ or 0) for extreme ratios. The influence of μ is particularly evident at intermediate ratios: for example, at $M_1/M_2 = 1.2$, increasing μ from 0.05 to 1.0 raises P_{M_1} from 0.71 to 0.81.

These results demonstrate that migration consistently drives agents toward resource-rich areas, with the degree of concentration increasing with both resource disparity and migration rate. Critically, such spatial sorting creates localized competition hotspots that may sustain high-effort strategies, highlighting the multi-scale nature of involution dynamics: global mixing coexists with local agglomeration.

3.3 Moderating role of resource abundance

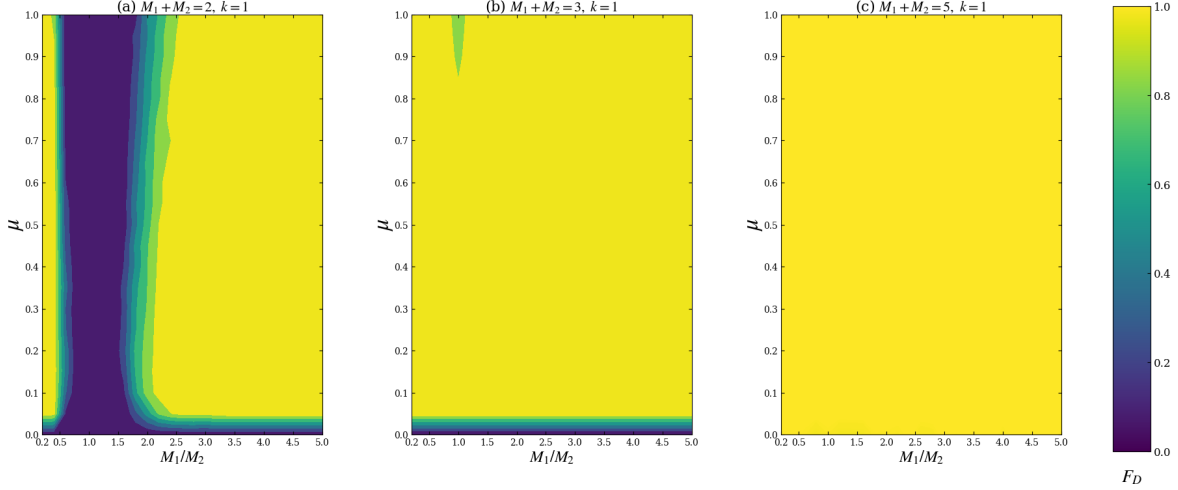


Figure 3: Proportion of competitive agents F_D as a function of the resource ratio M_1/M_2 and migration rate μ under different total resource endowments. Each panel corresponds to a fixed total resource $M_1 + M_2$ (2, 3, and 5, from left to right), with selection intensity fixed at $k = 1$. Color intensity represents the fraction of agents adopting the high-effort strategy D. Results are averaged over 50 independent runs on a 100×100 lattice with 2000 agents.

Figure 3 delineates the joint influence of total resource availability and spatial inequality on the prevalence of high-effort strategies. Three distinct regimes emerge as total resources increase from scarcity to abundance.

Resource scarcity ($M_1 + M_2 = 2.0$). In the absence of migration ($\mu = 0$), F_D remains uniformly zero across all resource ratios, indicating that without mobility, agents never adopt the high-effort strategy under scarcity. Once migration is permitted ($\mu > 0$), however, F_D becomes highly sensitive to the degree of resource inequality. For moderate ratios (M_1/M_2 between 2 and approximately 5), F_D remains low (typically below 0.2), suggesting that mild asymmetry does not trigger widespread involution. As the ratio increases beyond 5-10, F_D rises steadily, approaching 1 for extreme ratios ($M_1/M_2 > 15$). Notably, for any fixed M_1/M_2 , varying μ has negligible impact on F_D ; the critical distinction is simply whether migration exists or not. Thus, under resource scarcity, mobility enables agents to concentrate in richer areas, but the resulting involution intensity is governed primarily by the magnitude of resource disparity rather than by the migration rate itself.

Moderate resources ($M_1 + M_2 = 3.0$). At $\mu = 0$, F_D is again zero across all ratios, reaffirming that without migration, involution does not arise. However, for any $\mu > 0$, F_D jumps to near-unity for almost the entire parameter space. The only deviations occur at the lowest ratios (M_1/M_2 around 1-1.5), where F_D dips slightly to approximately 0.8-0.9. This suggests that once resources reach a certain threshold, the presence of migration alone suffices to drive nearly universal adoption of the high-effort strategy, regardless of the precise degree of inequality. The migration rate μ again plays a secondary role, with its exact value having little effect on the final outcome.

Resource abundance ($M_1 + M_2 = 5.0$). Here, F_D is uniformly close to 1 across all combinations of μ and M_1/M_2 , including at $\mu = 0$. Even without migration, resource abundance alone is sufficient to push the entire population toward the high-effort strategy. Mobility, whether present or not, exerts no discernible influence on the equilibrium.

Taken together, these results reveal a hierarchical control of involution by total resource availability: scarcity permits involution only under extreme inequality and requires migration; moderate abundance makes involution pervasive once migration is possible; abundance renders involution unconditional, independent of both mobility and spatial distribution. Across all regimes, the migration rate μ itself has minimal impact—only the presence or absence of migration matters. The key conclusion is that policy interventions aimed at mitigating involution should prioritize addressing total resource levels and spatial disparities over merely facilitating mobility.

3.4 Role of utility multiplier β

The parameter β scales the utility of high effort relative to low effort, with $u_D = \beta e_D$ and $e_D = 0.2$ fixed. We systematically varied β from 0.5 to 1.5 while keeping other parameters constant ($k = 1.0$, $\mu = 1.0$, 2000 agents). Figure 4 presents the results for three total resource levels ($M_1 + M_2 = 2.0, 3.0, 5.0$), each showing both the fraction of high-effort agents F_D and the fraction of agents located in region M_1 , P_{M_1} , as functions of the resource ratio M_1/M_2 and β .

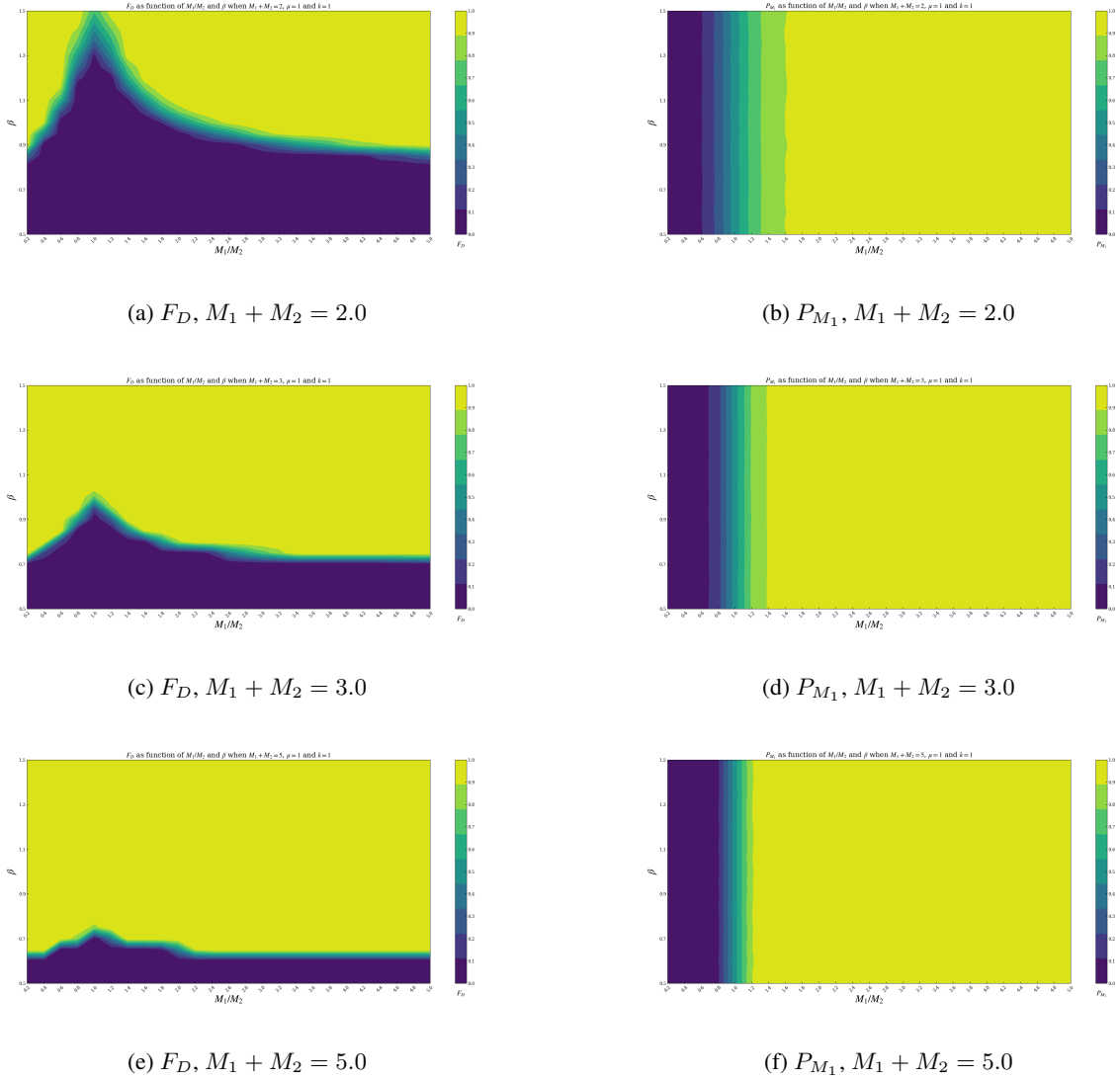


Figure 4: Effect of utility multiplier β on involution and spatial distribution for three total resource levels. Each pair of panels corresponds to a fixed total resource: (a,b) $M_1 + M_2 = 2.0$, (c,d) $M_1 + M_2 = 3.0$, (e,f) $M_1 + M_2 = 5.0$. Simulations with $k = 1.0$, $\mu = 1.0$, 2000 agents, averaged over 50 independent runs.

Figure 4 reveals that β acts as a key tuning parameter for involution, with its effect strongly modulated by total resource availability. At low total resources ($M_1 + M_2 = 2.0$, panels a and b), β must exceed a threshold of approximately 0.85 for high-effort adoption to emerge at all. Below this threshold, F_D remains zero across all resource ratios, indicating that the payoff advantage of high effort is insufficient to overcome its cost, even under extreme resource asymmetry. Once β surpasses this threshold, F_D begins to rise, but only for sufficiently large M_1/M_2 (or its reciprocal). For example, at $\beta = 0.9$, F_D exceeds 0.5 only when $M_1/M_2 > 3.0$ or < 0.33 ; at $\beta = 1.0$, the threshold shifts to approximately $M_1/M_2 > 2.0$ or < 0.5 . At the highest β values (≥ 1.3), F_D approaches 1.0 for all but the most balanced ratios near unity. The spatial distribution P_{M_1} mirrors this behavior: at low β , agents remain nearly evenly distributed ($P_{M_1} \approx 0.5$) regardless of resource ratio, because the low payoff of high effort discourages migration to the richer region. As β

increases, agents concentrate more strongly in the resource-rich region, with P_{M_1} approaching 1.0 for $M_1/M_2 > 1$ and 0.0 for $M_1/M_2 < 1$, and the transition sharpens with increasing β .

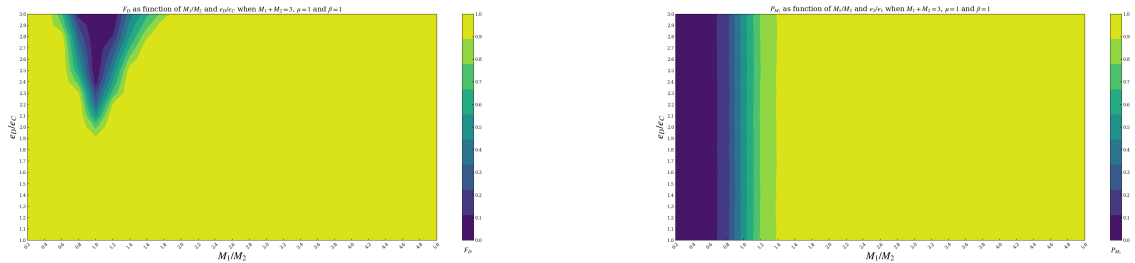
At moderate total resources ($M_1 + M_2 = 3.0$, panels c and d), the system exhibits a more abrupt transition. For $\beta \leq 0.7$, F_D is zero across all ratios, again indicating that low β suppresses involution entirely. At $\beta = 0.75$, F_D jumps to near-unity for extreme ratios ($M_1/M_2 > 3.0$ or < 0.33), while remaining low near symmetry. As β increases further, the range of ratios supporting high F_D expands rapidly: at $\beta = 0.8$, $F_D > 0.9$ for all $M_1/M_2 \geq 1.8$ or ≤ 0.56 ; at $\beta = 0.85$, the region of low F_D shrinks to a narrow band around $M_1/M_2 = 1$; and for $\beta \geq 0.9$, F_D is uniformly 1.0 across the entire parameter space. This indicates a sharp threshold: once β exceeds a critical value (approximately 0.85 at this resource level), the entire population adopts the high-effort strategy regardless of resource distribution. The spatial distribution P_{M_1} shows a corresponding pattern: at low β , agents are evenly spread; as β crosses the threshold, concentration in the richer region becomes extreme, with P_{M_1} approaching its extreme values rapidly, confirming that the decisions to adopt high effort and to migrate are tightly coupled.

When resources are abundant ($M_1 + M_2 = 5.0$, panels e and f), the influence of β is less dramatic but still discernible. At the lowest β values (0.5–0.6), F_D is already non-zero for moderately asymmetric ratios: for example, at $\beta = 0.5$, $F_D \approx 0.5$ at $M_1/M_2 = 1.0$ and rises to near 1.0 for ratios above 1.5 or below 0.67. As β increases, the range of ratios supporting high F_D expands, and the transition becomes sharper. At $\beta = 0.7$, F_D is already 1.0 for all ratios except those very close to unity. For $\beta \geq 0.75$, F_D is uniformly 1.0 across the entire parameter space, indicating that abundance combined with even a modest β suffices to drive universal involution. The spatial distribution P_{M_1} shows that even at the lowest β , agents concentrate strongly in the richer region when M_1/M_2 deviates from unity, reflecting the strong pull of abundant resources regardless of the payoff multiplier. As β increases, this concentration becomes even more pronounced, with P_{M_1} approaching its extreme values more rapidly.

In summary, β serves as a critical determinant of involution, exhibiting a clear threshold behavior that depends on total resource availability. Low β (below approximately 0.7–0.8) suppresses high-effort adoption entirely unless resources are both abundant and highly asymmetric. As β increases, a sharp transition occurs beyond which the population switches abruptly to universal high effort, with the threshold occurring at lower β when resources are more abundant. The spatial concentration of agents in the richer region closely tracks this strategy shift, indicating that migration and strategy choice are mutually reinforcing. These findings underscore that policies aimed at reducing involution should consider not only the total resource pool and its spatial distribution, but also the effective payoff multiplier—which in real-world contexts could be influenced by factors such as tax rates, wage floors, or effort caps.

3.5 Effect of effort ratio e_D/e_C

We also varied the effort levels while keeping utilities proportional to efforts (i.e., $u_i = e_i$). Figure 5 presents the results for different effort ratios e_D/e_C (where $e_C = 0.1$, e_D varied) under fixed total resources $M_1 + M_2 = 3.0$, migration rate $\mu = 1.0$, and selection intensity $k = 1.0$. Panel (a) shows the fraction of high-effort agents F_D as a function of the effort ratio for several representative resource ratios M_1/M_2 , while panel (b) displays F_D as a function of M_1/M_2 for various effort ratios.



(a) F_D vs. e_D/e_C for various M_1/M_2

(b) F_D vs. M_1/M_2 for various e_D/e_C

Figure 5: Effect of the effort ratio e_D/e_C on involution. Simulations with $M_1 + M_2 = 3.0$, $\mu = 1.0$, $k = 1.0$, and 2000 agents, averaged over 50 independent runs.

Figure 5 reveals that the effort ratio e_D/e_C critically modulates the conditions under which involution emerges. When the effort ratio is close to unity ($e_D/e_C \approx 1.0$), high effort is only slightly more costly than low effort, and F_D remains uniformly high (near 1.0) across all resource ratios M_1/M_2 . As the effort ratio increases, making high effort progressively more expensive, a distinct trough appears around the symmetric point $M_1/M_2 = 1.0$. For instance,

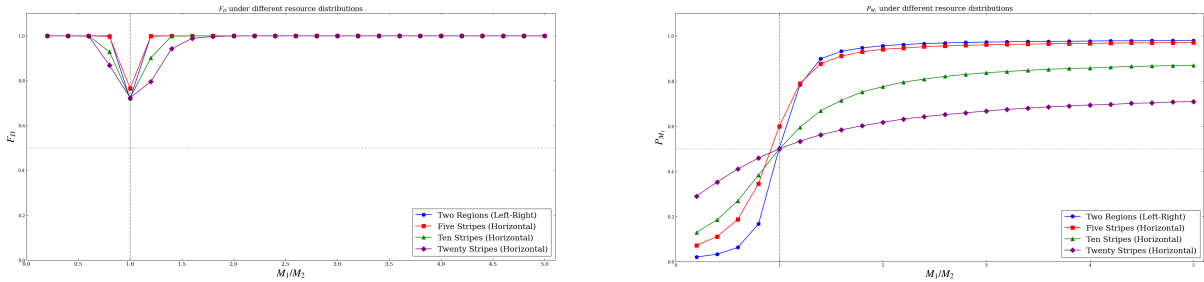
at $e_D/e_C = 2.0$, F_D drops to approximately 0.75 at $M_1/M_2 = 1.0$, while still exceeding 0.99 at $M_1/M_2 = 0.8$ and 1.2. As the effort ratio rises further, the central trough deepens and widens: at $e_D/e_C = 2.5$, F_D falls below 0.01 at the symmetric point, but remains above 0.94 at $M_1/M_2 = 1.4$; at $e_D/e_C = 3.0$, F_D is essentially zero for $0.8 \lesssim M_1/M_2 \lesssim 1.2$, while approaching unity for ratios below 0.6 or above 1.6. The curves exhibit clear symmetry about $M_1/M_2 = 1$ (on a logarithmic scale), confirming that the system responds identically to swapping the two regions.

The spatial distribution P_{M_1} (data not shown) mirrors these trends. For low effort ratios, agents concentrate strongly in the richer region whenever $M_1/M_2 \neq 1$. As the effort ratio increases, the degree of concentration near the symmetric point diminishes, with P_{M_1} approaching 0.5 for $M_1/M_2 \approx 1$, indicating that the high cost of effort discourages migration when resource gains are marginal. However, for extreme resource ratios, P_{M_1} remains close to 0 or 1, reflecting the persistent pull of abundant resources.

In essence, the effort ratio sets a threshold for involution: the greater the relative cost of high effort, the larger the resource asymmetry required to sustain it. In policy terms, measures that increase the effective cost of excessive effort (e.g., progressive taxation on overtime, strict working hour limits) can curb involution by raising the bar for when competition becomes worthwhile, even without altering the underlying resource distribution.

3.6 Influence of resource distribution patterns

Resource distribution is not always a simple step function. To explore the effect of spatial mixing, we simulated configurations with alternating stripes of two resource levels. The number of stripes (two, five, ten, twenty) represents the degree of mixing: more stripes correspond to finer-grained alternation and thus higher spatial heterogeneity at the local scale. Figure 6 presents the results.



(a) Fraction of high-effort agents F_D as a function of M_1/M_2 for different stripe patterns.

(b) Fraction of agents located in the M_1 region P_{M_1} as a function of M_1/M_2 for different stripe patterns.

Figure 6: Effect of resource mixing on involution and spatial distribution. Simulations with total resources $M_1 + M_2 = 3.0$, migration rate $\mu = 1.0$, selection intensity $k = 1.0$, and 2000 agents. Each curve is averaged over 50 independent runs.

Figure 6a shows that increasing the degree of mixing (more stripes) systematically reduces the prevalence of the high-effort strategy for a given resource ratio, except in the immediate vicinity of $M_1/M_2 = 1$ where F_D remains largely unchanged. For example, at $M_1/M_2 = 0.8$, F_D drops from nearly 1.0 in the two-region case to about 0.87 for twenty stripes; a similar decline is observed at $M_1/M_2 = 1.2$. This indicates that spatial fragmentation mitigates involution by providing agents with more balanced local environments, thereby weakening the incentive to escalate effort.

Figure 6b examines how mixing affects agent distribution. In the two-region setup, agents strongly concentrate in the richer region: when $M_1/M_2 < 1$, P_{M_1} is very low (most agents leave the poorer M_1 region); when $M_1/M_2 > 1$, P_{M_1} approaches 1. As stripes become finer, this polarisation diminishes: P_{M_1} moves closer to 0.5 for all resource ratios, indicating a more uniform spatial distribution. Finer mixing thus reduces the tendency of agents to flock to the resource-rich area, which in turn lowers local competitive pressure and contributes to the suppression of F_D seen in panel (a).

Together, these results demonstrate that even without altering the global resource totals, the way resources are arranged spatially can significantly influence both the intensity of involution and the distribution of agents. The key insight is that spatial fragmentation serves as a powerful tool to mitigate excessive competition, suggesting that policies promoting mixing of different resource levels (e.g., through urban planning or economic diversification) may help alleviate involution.

3.7 Impact of agent population size

The number of agents (i.e., population density) modulates the intensity of local competition and spatial sorting. Figure 7 examines the effect of varying the total number of agents from 2000 to 8000 (corresponding to densities $\rho = 0.2$ to 0.8) while keeping the lattice size fixed (100×100). Panel (a) shows the fraction of agents located in the M_1 region, P_{M_1} , as a function of the resource ratio M_2/M_1 for different agent numbers. Panel (b) displays the fraction of high-effort agents, F_D , as a function of agent number for several representative values of M_2/M_1 , highlighting how population density influences the propensity to adopt the competitive strategy.

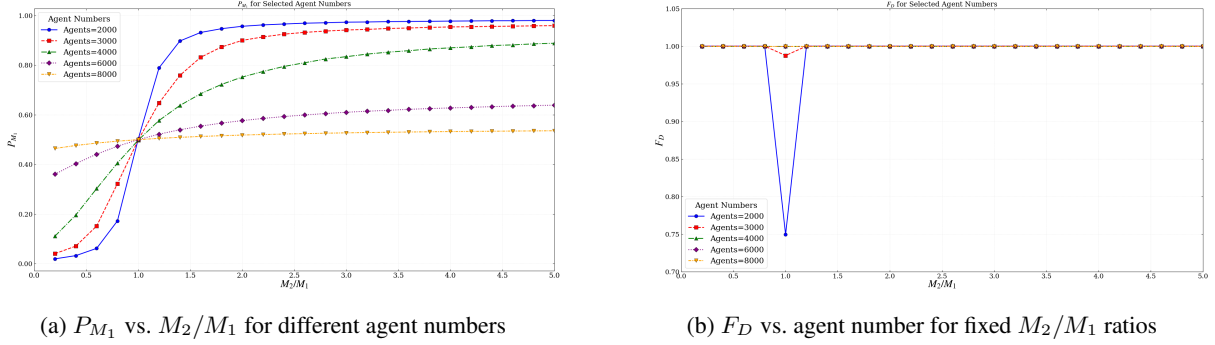


Figure 7: Effect of population size on spatial distribution and involution. Simulations with total resources $M_1 + M_2 = 3.0$, migration rate $\mu = 1.0$, selection intensity $k = 1.0$, and 50 independent runs per condition.

Figure 7a reveals that spatial concentration in the richer region is strongly affected by both resource asymmetry and population density. When $M_2/M_1 < 1$ (i.e., M_1 is the poorer region), P_{M_1} is very low for small populations, indicating that most agents abandon the poorer region. As density increases, however, P_{M_1} rises markedly, approaching 0.5 for the highest densities even at extreme ratios. For example, at $M_2/M_1 = 0.2$ (i.e., $M_1/M_2 = 5$), P_{M_1} increases from about 0.02 for 2000 agents to nearly 0.46 for 8000 agents. This trend demonstrates that crowding in the resource-rich region forces some agents to remain in or move to the poorer area, thereby reducing spatial inequality. The same pattern holds symmetrically when $M_2/M_1 > 1$ (with M_1 being the richer region), where P_{M_1} decreases toward 0.5 as density grows.

Figure 7b illustrates how population density affects the adoption of the high-effort strategy. For resource ratios sufficiently far from unity (e.g., $M_2/M_1 = 0.5$ or 2.0), F_D is uniformly 1.0 regardless of agent number, indicating that extreme resource asymmetry alone suffices to drive the entire population toward involution. In contrast, near the symmetric point $M_2/M_1 = 1.0$, F_D exhibits a clear dependence on density: it increases from approximately 0.75 for 2000 agents to 0.99 for 3000 agents and reaches 1.0 for larger populations. Thus, higher population density intensifies competition even when resources are evenly distributed, pushing the system toward universal high effort.

Taken together, these results show that population density has contrasting effects on spatial distribution and strategic choice. On one hand, higher density promotes a more balanced spatial distribution by saturating attractive regions and forcing agents to occupy less favorable areas. On the other hand, it exacerbates involution by increasing local competitive pressure, particularly in situations where resources are nearly equal. The net outcome is that while agents become more evenly spread, they all tend to adopt the high-effort strategy, leading to widespread involution irrespective of spatial equity. This highlights a fundamental trade-off: policies that increase population density may improve spatial equity but at the cost of intensifying overall competition.

3.8 Synthesis and policy implications

Collectively, our results reveal a nuanced picture: migration plays a dual and context-dependent role: it enables agents to relocate toward resource-rich areas, creating local competition hotspots, while its effect on global involution intensity is primarily mediated by total resource abundance rather than the migration rate itself. Specifically, migration acts as a precondition for involution under resource scarcity, triggers near-universal high-effort adoption under moderate resources, and becomes irrelevant under abundance. In particular:

- Enhancing mobility (e.g., through job platforms, relocation subsidies) can help agents escape saturated markets, but without addressing resource disparities it merely shifts competition.
- Reducing resource inequality between regions prevents the formation of extreme concentration and the associated local involution.

- Fragmentation of resource patches (e.g., mixing high- and low-resource zones) can lower involution even without changing total resources.
- Policy interventions should be tailored to the resource context: mobility works best when resources are adequate, but may have limited impact under extreme scarcity.

In summary, our analysis demonstrates that the interplay between migration, resource distribution, and population density determines the intensity and spatial pattern of involution. The most effective policies are those that simultaneously address resource disparities and mobility, while considering the prevailing resource abundance.

4 Theoretical Analysis

To gain deeper insight into the simulation results, we develop a mean-field approximation of the model. This approach neglects spatial correlations and local fluctuations, assuming that agents are uniformly distributed within each region and that interactions are well-mixed. Despite its simplifications, the mean-field theory captures the essential mechanisms driving migration and strategy evolution, and provides analytical predictions for the asymptotic behavior of the system.

4.1 Mean-Field Payoffs

Let $\rho = N_{\text{agents}}/N^2$ denote the global density of agents. Define F_D as the fraction of agents adopting the high-effort strategy D, and P_{M_1} as the fraction of agents located in region M_1 (the complementary fraction $1 - P_{M_1}$ resides in region M_2). The average utility in the whole population is

$$\bar{u} = F_D u_D + (1 - F_D) u_C, \quad (5)$$

where $u_C = e_C$ and $u_D = \beta e_D$, with β being the utility multiplier for the high-effort strategy.

Consider an agent of type $i \in \{C, D\}$ located in region $r \in \{1, 2\}$ with resource level M_r . Under the mean-field approximation, the expected payoff per competition (i.e., the average over the five lattice sites the agent participates in) is given by

$$\mathbb{E}[\pi_i^r] = M_r \frac{u_i}{u_i + 4\rho\bar{u}} - e_i. \quad (6)$$

The derivation is as follows: at each of the five sites, the agent competes with the occupants of the four neighboring sites. The expected total utility competing at that site is u_i (the focal agent's own utility) plus $4\rho\bar{u}$ (the expected utility from the four neighbors, each occupied with probability ρ and having average utility \bar{u}). Hence the agent's share of the resource M_r is $M_r \cdot u_i / (u_i + 4\rho\bar{u})$. Summing over five sites and dividing by five gives the average payoff per competition. The cost term $-e_i$ reflects that the agent expends its full effort e_i in each competition, resulting in a total cost of $5e_i$ over five competitions, which averages to e_i per competition.

The average payoff in region r is obtained by averaging over the two strategies:

$$\mathbb{E}[\pi_r] = F_D \mathbb{E}[\pi_D^r] + (1 - F_D) \mathbb{E}[\pi_C^r]. \quad (7)$$

Substituting Eq. (6) yields

$$\mathbb{E}[\pi_r] = M_r H(\bar{u}) - [F_D e_D + (1 - F_D) e_C], \quad (8)$$

where we have introduced the auxiliary function

$$H(\bar{u}) = F_D \frac{u_D}{u_D + 4\rho\bar{u}} + (1 - F_D) \frac{u_C}{u_C + 4\rho\bar{u}}. \quad (9)$$

Since $u_D > u_C > 0$, we have $H(\bar{u}) > 0$ for all $\bar{u} > 0$.

4.2 Migration Dynamics

The migration process described in Sec. 2 implies that agents compare payoffs and tend to move toward regions offering higher returns. Under the mean-field approximation, the evolution of the spatial distribution P_{M_1} can be described by the following differential equation [29, 30, 31]:

$$\frac{dP_{M_1}}{dt} = \mu P_{M_1} (1 - P_{M_1}) \tanh \left[\frac{k}{2} (\mathbb{E}[\pi_{M_1}] - \mathbb{E}[\pi_{M_2}]) \right], \quad (10)$$

where μ is the migration rate and k the selection intensity. This form arises from the pairwise comparison rule: the probability that an agent in the poorer region moves to the richer region is proportional to \tanh of the payoff difference,

and the factor $P_{M_1}(1 - P_{M_1})$ captures the fraction of agents that are potentially mobile (those in the less attractive region) and the availability of empty sites in the more attractive region.

Using Eq. (8), the payoff difference simplifies to

$$\mathbb{E}[\pi_{M_1}] - \mathbb{E}[\pi_{M_2}] = (M_1 - M_2)H(\bar{u}), \quad (11)$$

because the cost terms cancel. Substituting into Eq. (10) gives

$$\frac{dP_{M_1}}{dt} = \mu P_{M_1}(1 - P_{M_1}) \tanh\left[\frac{k}{2}(M_1 - M_2)H(\bar{u})\right]. \quad (12)$$

Since $H(\bar{u}) > 0$, the sign of the argument inside the hyperbolic tangent is determined solely by $M_1 - M_2$. Consequently, we obtain the following result:

Proposition 1 (Migration equilibrium) *Under the mean-field dynamics (12), the system exhibits:*

- If $M_1 > M_2$, then $dP_{M_1}/dt > 0$ for all $0 < P_{M_1} < 1$, implying that P_{M_1} increases monotonically and converges to 1 (all agents concentrate in region M_1).
- If $M_1 < M_2$, then $dP_{M_1}/dt < 0$ for all $0 < P_{M_1} < 1$, and P_{M_1} decreases to 0 (all agents concentrate in region M_2).
- If $M_1 = M_2$, then $dP_{M_1}/dt = 0$ for any $P_{M_1} \in [0, 1]$; the system is neutrally stable and any initial distribution persists.

Thus, any asymmetry in regional resources inevitably drives the population toward complete agglomeration in the more resource-abundant region.

4.3 Strategy Dynamics

The evolution of the fraction F_D of high-effort agents is governed by a replicator-type equation derived from the pairwise comparison rule [29, 30, 31]:

$$\frac{dF_D}{dt} = F_D(1 - F_D) \tanh\left[\frac{k}{2}(\mathbb{E}[\pi_D] - \mathbb{E}[\pi_C])\right]. \quad (13)$$

The average payoff for a strategy i , $\mathbb{E}[\pi_i]$, is obtained by averaging over regions:

$$\mathbb{E}[\pi_i] = P_{M_1}\mathbb{E}[\pi_i^{M_1}] + (1 - P_{M_1})\mathbb{E}[\pi_i^{M_2}]. \quad (14)$$

Using Eq. (6) and introducing the region-averaged resource $\bar{M} = P_{M_1}M_1 + (1 - P_{M_1})M_2$, we obtain

$$\mathbb{E}[\pi_i] = \bar{M} \frac{u_i}{u_i + 4\rho\bar{u}} - e_i. \quad (15)$$

Define the payoff difference $\Delta\pi = \mathbb{E}[\pi_D] - \mathbb{E}[\pi_C]$. From Eq. (15),

$$\Delta\pi = \bar{M}\Phi(\bar{u}) - \Delta e, \quad (16)$$

where $\Delta e = e_D - e_C > 0$ and

$$\Phi(\bar{u}) = \frac{u_D}{u_D + 4\rho\bar{u}} - \frac{u_C}{u_C + 4\rho\bar{u}} = \frac{4\rho(u_D - u_C)\bar{u}}{(u_D + 4\rho\bar{u})(u_C + 4\rho\bar{u})}. \quad (17)$$

Note that $\Phi(0) = 0$, $\Phi(\bar{u}) > 0$ for $\bar{u} > 0$, and Φ is a unimodal function achieving its maximum at $\bar{u}_{\max} = \sqrt{u_C u_D}/(4\rho)$.

The fixed points of Eq. (13) are $F_D = 0$, $F_D = 1$, and any F_D satisfying $\Delta\pi = 0$. The stability of these fixed points is determined by the sign of $\Delta\pi$ in their vicinity. Specifically, $F_D = 0$ is stable if $\Delta\pi < 0$ for F_D near 0, and $F_D = 1$ is stable if $\Delta\pi > 0$ for F_D near 1. An interior fixed point exists only when $\Delta\pi = 0$ has a solution $F_D^* \in (0, 1)$; its stability depends on the derivative of $\Delta\pi$ with respect to F_D .

For the parameter values used in our simulations ($e_C = 0.1$, $e_D = 0.2$, $\beta = 1$, $\rho = 0.2$), we have $u_C = 0.1$, $u_D = 0.2$, and $4\rho\bar{u} = 0.8\bar{u}$. The maximum of Φ occurs at $\bar{u}_{\max} = \sqrt{0.1 \times 0.2}/0.8 \approx 0.1768$, with $\Phi_{\max} \approx 0.1710$. At the boundaries,

$$\begin{aligned} F_D = 0 &\Rightarrow \bar{u} = u_C = 0.1, & \Phi(0.1) &\approx 0.1587, \\ F_D = 1 &\Rightarrow \bar{u} = u_D = 0.2, & \Phi(0.2) &\approx 0.1710. \end{aligned}$$

Thus $\Phi_{\min} = \min\{\Phi(0.1), \Phi(0.2)\} = 0.1587$.

The interior equilibrium condition $\Delta\pi = 0$ reduces to

$$\bar{M}\Phi(\bar{u}) = \Delta e = 0.1. \quad (18)$$

Consequently, an interior equilibrium exists only when the average resource \bar{M} lies in the interval

$$\frac{0.1}{\Phi_{\max}} \leq \bar{M} \leq \frac{0.1}{\Phi_{\min}} \iff 0.585 \approx \frac{0.1}{0.1710} \leq \bar{M} \leq \frac{0.1}{0.1587} \approx 0.630. \quad (19)$$

Proposition 2 (Strategy equilibria) *For the given parameters:*

- If $\bar{M} < 0.585$, then $\Delta\pi < 0$ for all $F_D \in [0, 1]$; hence $F_D = 0$ is globally stable (all agents adopt low effort).
- If $\bar{M} > 0.630$, then $\Delta\pi > 0$ for all $F_D \in [0, 1]$; hence $F_D = 1$ is globally stable (all agents adopt high effort).
- If $0.585 < \bar{M} < 0.630$, there exist two interior fixed points: one unstable and one stable. The stable interior fixed point corresponds to a mixed-strategy equilibrium where both strategies coexist. However, due to the narrowness of this interval, such coexistence is rare and requires precise tuning of parameters.

4.4 Coupling of Migration and Strategy

The two dynamical subsystems are coupled through the average resource $\bar{M} = P_{M_1}M_1 + (1 - P_{M_1})M_2$, which depends on the spatial distribution, and the average utility \bar{u} , which depends on the strategy composition. Proposition 1 shows that migration drives P_{M_1} to either 0 or 1 whenever $M_1 \neq M_2$. Consequently, \bar{M} converges to the resource level of the richer region. Unless the two resource levels are very close (so that \bar{M} falls inside the narrow coexistence interval), the strategy dynamics will then drive F_D to the corresponding boundary equilibrium. This explains why the simulation results predominantly exhibit homogeneous strategy adoption (all C or all D) when resource asymmetry is present. Only when resources are nearly equal and the migration-driven concentration is weak can mixed strategies persist.

These mean-field predictions are in excellent qualitative agreement with the simulation outcomes presented in Sec. 3, validating the theoretical framework and providing a mechanistic understanding of the observed involution dynamics.

5 Discussion and Conclusion

5.1 Discussion

This study constructs and analyzes an evolutionary game model of involution that integrates agent migration and spatial resource heterogeneity, which extends the existing theoretical framework and vividly depicts the real-world competitive dynamics of **food delivery riders** and **homogeneous physical stores**. By combining strategy updating and cross-regional mobility, this research reveals the internal mechanism of how spatial resources and migration behavior dominate the evolutionary trend of involution.

The theoretical analysis based on mean-field approximation and numerical simulations reveal four core findings with strong empirical relevance. First, resource disparity dominates the migration direction of agents, which is highly consistent with the agglomeration phenomenon in practical scenarios. Food delivery riders tend to gather in commercial districts and residential areas with sufficient order resources, while homogeneous stores such as milk tea shops and convenience stores cluster in regions with large passenger flow. Rational agents continuously flow into high-resource areas until the intensification of competition offsets the regional resource advantages, forming a spatial agglomeration pattern driven by profit differentials.

Second, the coupling of migration and strategy evolution pushes the system toward an extreme equilibrium, which explains the persistent involution dilemma of the two typical groups. For food delivery riders, regional agglomeration widens the payoff gap between high-effort and low-effort strategies, forcing riders to extend working hours and scramble orders involuntarily. For homogeneous stores, agglomeration triggers homogenized competition, forcing stores to increase investment in promotion and price reduction to maintain competitiveness. The results confirm that stable coexistence of high and low effort only exists in a narrow range of average resources, and spatial migration caused by resource heterogeneity makes moderate competition difficult to maintain.

Third, resource abundance has a non-monotonic effect on involution. Simply increasing regional resources (e.g., rising order volume, growing passenger flow) fails to alleviate involution. Instead, it further stimulates the proliferation of

high-effort strategies and accelerates the evolution to full involution, which explains why severe involution is more prevalent in prosperous business districts.

Fourth, mobility acts as a double-edged sword. Increasing migration propensity helps agents escape locally saturated markets, but it only transfers the competition from low-resource areas to high-resource areas without resolving the root cause of involution. Only the coordinated governance of balancing spatial resource distribution and regulating excessive competition can effectively curb involution.

In terms of practical implications, targeted interventions are proposed for the two scenarios. For the food delivery industry, regulators should optimize order allocation algorithms, set reasonable working hour limits and guarantee minimum income per order to narrow the payoff gap of excessive effort. For homogeneous physical stores, policies should guide the balanced layout of commercial resources, encourage differentiated operations and reduce blind agglomeration and inefficient competition.

5.2 Limitations and Future Work

Despite the contributions of this study, several limitations should be addressed in future research. First, the mean-field analysis ignores spatial correlations and network interaction topologies. Future research can introduce small-world or scale-free networks to simulate the interaction patterns of delivery riders and stores more realistically.

Second, the two-region setting and fixed total population are simplified assumptions. Expanding the model to multi-region scenarios with dynamically changing resources and variable population size will better fit the long-term evolutionary laws of real markets.

Third, the model adopts discrete high/low effort strategies, while effort levels of riders and investment intensity of stores are continuous variables in reality. A continuous strategy space can depict the gradual evolution of involution more precisely.

Fourth, the migration rate is set as a fixed parameter. Introducing adaptive migration rules based on experience learning and social information can capture the complex feedback between mobility and strategy selection.

5.3 Conclusion

This study systematically explores the evolutionary mechanism of involution by incorporating spatial resource heterogeneity and agent migration into the evolutionary game framework. The results demonstrate that spatial resource disparity triggers directed agent agglomeration, and the coupling of migration and strategy evolution drives the system to converge to a homogeneous high-effort equilibrium, making moderate competition unsustainable. Mobility alone transfers rather than eliminates involution, and unilateral resource expansion may intensify excessive competition.

These findings provide a solid theoretical explanation for the involution phenomenon of food delivery riders and homogeneous physical stores, and clarify the key role of spatial factors in competitive dynamics. The research not only enriches the application of evolutionary game theory in socio-economic systems, but also provides decision-making support for regulating platform competition, protecting the rights and interests of practitioners, and optimizing the layout of commercial space.

This work serves as a foundation for exploring the complex interaction between competition, mobility and resource allocation, and offers a new analytical perspective for governing involution in various competitive scenarios.

Acknowledgements

This work was supported by the Wuhan City Polytechnic Research Project (Grant No. 2025WHCPB02) and the National Natural Science Foundation of China (Grant No. 72231010).

References

- [1] Yuan Tao, Yanping Lu, Wei Shi, and Guangzhe Frank Yuan. Multidimensional diagnostic features and intervention pathways for youth mental disorders in china's involution society. *Asian Journal of Psychiatry*, 108:104531, 2025. ISSN 1876-2018. doi:<https://doi.org/10.1016/j.ajp.2025.104531>. URL <https://www.sciencedirect.com/science/article/pii/S1876201825001741>.
- [2] Chaoqian Wang, Chaochao Huang, Qihui Pan, and Mingfeng He. Modeling the social dilemma of involution on a square lattice. *Chaos, Solitons & Fractals*, 158:112092, 2022. ISSN 0960-

0779. doi:<https://doi.org/10.1016/j.chaos.2022.112092>. URL <https://www.sciencedirect.com/science/article/pii/S0960077922003022>.
- [3] Yi Xiong. Understanding China’s “Anti-involution” Drive. Deutsche Bank Research Institute. URL <https://www.dbresearch.com/PROD/RI-PROD/PDFVIEWER.calias?pdfViewerPdfUrl=PROD000000000603307>. Chief Economist, Ph.D.
- [4] Martin A. Nowak and Robert M. May. Evolutionary games and spatial chaos. *Nature*, 359(6398):826–829, October 1992. doi:10.1038/359826A0.
- [5] György Szabó and Csaba Tóke. Evolutionary prisoner’s dilemma game on a square lattice. *Physical Review E*, 58(1):69–73, October 1997. doi:10.1103/PHYSREVE.58.69.
- [6] Attila Szolnoki, Matjaž Perc, György Szabó, and Hans-Ulrich Stark. Impact of aging on the evolution of cooperation in the spatial prisoner’s dilemma game. *Physical Review E*, 80(2):021901, August 2009. doi:10.1103/PHYSREVE.80.021901.
- [7] Feng Zhang, Yan-Ping Liu, Yan-Ping Liu, Rui-Wu Wang, and Si-Yi Wang. Super-rational aspiration induced strategy updating promotes cooperation in the asymmetric prisoner’s dilemma game. *Applied Mathematics and Computation*, 403:126180, August 2021. doi:10.1016/J.AMC.2021.126180.
- [8] Matjaž Perc, Jesús Gómez-Gardenes, Attila Szolnoki, Luis M Floría, and Yamir Moreno. Evolutionary dynamics of group interactions on structured populations: a review. *Journal of the Royal Society Interface*, 10(80):20120997–20120997, March 2013. doi:10.1098/RSIF.2012.0997.
- [9] Oliver P. Hauser, Christian Hilbe, Krishnendu Chatterjee, and Martin A. Nowak. Social dilemmas among unequals. *Nature*, 572(7770):524–527, August 2019. doi:10.1038/S41586-019-1488-5.
- [10] Vito Latora, Vito Latora, Vito Latora, Yamir Moreno, Yamir Moreno, Guilherme Ferraz de Arruda, Federico Battiston, Federico Battiston, Matjaž Perc, Matjaž Perc, and Unai Alvarez-Rodriguez. Evolutionary dynamics of higher-order interactions in social networks. *Nature Human Behaviour*, 5(5):586–595, January 2021. doi:10.1038/S41562-020-01024-1.
- [11] Chaoqian Wang and Attila Szolnoki. Involution game with spatio-temporal heterogeneity of social resources. *Applied Mathematics and Computation*, 430:127307, 2022. ISSN 0096-3003. doi:<https://doi.org/10.1016/j.amc.2022.127307>. URL <https://www.sciencedirect.com/science/article/pii/S0096300322003812>.
- [12] Bo Li. Involution game with specialization strategy. *Advances in Complex Systems*, 26(07n08):2350013, 2023.
- [13] Chaochao Huang and Chaoqian Wang. Memory-based involution dilemma on square lattices. *Chaos, Solitons & Fractals*, 178:114384–114384, January 2024.
- [14] He Chaocheng, Huang Qian, Li Xinru, Zuo Renxian, Liu Fuzhen, Wei Yuchi, and Wu Jiang. Involution-cooperation-lying flat game on a network-structured population in the group competition. *IEEE Transactions on Computational Social Systems*, July 2023. doi:10.1109/TCSS.2023.3287772.
- [15] Chaoqian Wang and Chaochao Huang. Between local and global strategy updating in public goods game. *Physica A: Statistical Mechanics and its Applications*, 606:128097, 2022. ISSN 0378-4371. doi:<https://doi.org/10.1016/j.physa.2022.128097>. URL <https://www.sciencedirect.com/science/article/pii/S0378437122006793>.
- [16] Liming Zhang, Haihong Li, Qionglin Dai, and Junzhong Yang. Migration based on environment comparison promotes cooperation in evolutionary games. *Physica A: Statistical Mechanics and its Applications*, 595:127073, 2022. ISSN 0378-4371. doi:<https://doi.org/10.1016/j.physa.2022.127073>. URL <https://www.sciencedirect.com/science/article/pii/S0378437122001224>.
- [17] Haihong Li, Qionglin Dai, Junzhong Yang, Lan Zhang, and Changwei Huang. Effects of directional migration for pursuit of profitable circumstances in evolutionary games. *Chaos Solitons & Fractals*, 144:110709, March 2021. doi:10.1016/J.CHAOS.2021.110709.
- [18] Allison K Shaw, Martha Torstenson, Meggan E Craft, and Sandra A Binning. Gaps in modelling animal migration with evolutionary game theory: infection can favour the loss of migration. *Philosophical Transactions of the Royal Society B*, 378(1876):20210506–20210506, May 2023. doi:10.1098/RSTB.2021.0506.
- [19] Pierre Buesser, Marco Tomassini, and Alberto Antonioni. Opportunistic migration in spatial evolutionary games. *Physical Review E*, 88(4):042806, October 2013. doi:10.1103/PHYSREVE.88.042806.
- [20] Shilin Xiao, Liming Zhang, Haihong Li, Qionglin Dai, and Junzhong Yang. Environment-driven migration enhances cooperation in evolutionary public goods games. *The European Physical Journal B*, 95(4):67, 2022.

-
- [21] Yan Li and Hang Ye. Effect of migration based on strategy and cost on the evolution of cooperation. *Chaos, Solitons & Fractals*, 76:156–165, July 2015. doi:10.1016/J.CHAOS.2015.04.006.
- [22] Sandeep Dhakal, Raymond Chiong, Manuel Chica, and The Anh Han. Evolution of cooperation and trust in an N-player social dilemma game with tags for migration decisions. *Royal Society Open Science*, 9(5):212000–212000, May 2022.
- [23] Xingping Sun, Kaiyu Feng, Hongwei Kang, Yong Shen, and Qingyi Chen. Adaptive migration guided by reputation-pheromone dynamics in spatial games. *Chaos, Solitons & Fractals*, 202:117440–117440, January 2026.
- [24] Yves Achdou, Pierre Cardaliaguet, François Delarue, Alessio Porretta, Filippo Santambrogio, Pierre Cardaliaguet, and Alessio Porretta. An Introduction to Mean Field Game Theory. pages 1–158, January 2020. doi:10.1007/978-3-030-59837-2_1.
- [25] William H Sandholm. *Evolutionary game theory*. Springer, 2020.
- [26] Dmitriy Antonov, Evgeni Burovski, and Lev Shchur. Mean-field interactions in evolutionary spatial games. *Physical Review Research*, 3(3):L032072–L032072, September 2021.
- [27] Arne Traulsen, Martin A. Nowak, and Jorge M. Pacheco. Stochastic dynamics of invasion and fixation. *Physical Review E*, 74(1):011909–011909, July 2006. doi:10.1103/PHYSREVE.74.011909.
- [28] Yong Shen, Yujie Ma, Hongwei Kang, Xingping Sun, and Qingyi Chen. Learning and propagation: Evolutionary dynamics in spatial public goods games through combined Q-learning and Fermi rule. *Chaos, Solitons & Fractals*, 187:115377–115377, October 2024.
- [29] Karl Sigmund and Josef Hofbauer. *Evolutionary games and population dynamics*. Cambridge University Press, January 1998.
- [30] Christoph Hauert and György Szabó. Game theory and physics. *American Journal of Physics*, 73(5):405–414, May 2005. doi:10.1119/1.1848514.
- [31] Martin A. Nowak. *Evolutionary Dynamics: Exploring the Equations of Life*. Harvard University Press, September 2006.